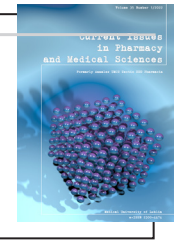
DOI: 10.2478/cipms-2022-0013 Curr. Issues Pharm. Med. Sci., Vol. 35, No. 2, Pages 67-74

sciendo

Current Issues in Pharmacy and Medical Sciences

Formerly ANNALES UNIVERSITATIS MARIAE CURIE-SKLODOWSKA, SECTIO DDD, PHARMACIA

journal homepage: http://www.curipms.umlub.pl/



Coumarin derivatives against amyloid-beta 40 – 42 peptide and *tau* protein

Joanna Kowalczyk[1], Krystyna Skalicka-Wozniak[2*], Barbara Budzynska[1], Nesrine El Sayed[3], Alba Espargaró[4,5], Raimon Sabate[4,5]

[1] Independent Laboratory of Behavioral Studies, Medical University of Lublin, Jaczewskiego 4, 20-090 Lublin, Poland
[2] Department of Natural Products Chemistry, Medical University of Lublin, 1 Chodzki Street, 20-093, Lublin, Poland
[3] Department of Pharmacology and Toxicology, Cairo University, Cairo Egypt
[4] Department of Pharmacy and Pharmaceutical Technology and Physical-Chemistry, University of Barcelona, Avda, Barcelona, Catalonia, Spain
[5] Institute of Nanoscience and Nanotechnology (IN2UB), University of Barcelona, Barcelona, Catalonia, Spain

ARTICLE INFO

Received 13 March 2022
Acceted 17 June 2022

Keywords:
neurodegeneration,
tau,
Aβ40/42,
in vitro,
in cellulo,
coumarins.

ABSTRACT

In preclinical studies, simple coumarins (scoparone, limettin) and furanocoumarins (imperatorin, xanthotoxin, bergapten) have already found to demonstrate procognitive abilities. This suggests that they hold antioxidative, anti-inflammatory and inhibitory action towards acetylcholinesterase activities. However, little is known about their influence on the amyloidal structure formation, the leading cause of Alzheimer's disease (AD). *In vitro* and *in cellulo* assays were applied to evaluate the effect of selected coumarins on the different stages of Aβ40/42 and *tau* protein aggregation. Kinetic analyses were performed to evaluate their inhibiting abilities in time. Limettin revealed the most potent inhibiting profile towards Aβ40 aggregation, however, all tested compounds presented low influence on Aβ42 and *tau* protein aggregation inhibition. Despite the preliminary stage of the project, the promising effects of coumarins on Aβ40 aggregation were shown. This suggests the coumarin scaffold can serve as a potential multitarget agent in AD treatment, but further studies are required to confirm this.

INTRODUCTION

Biotechnological methods, including the use of bacterial cells as *in cellulo* screening models, give a deeper insight into the processes inside the cell and are accessible for genetic modulation. Therefore, diseases with genetic background, such as APOE ε4-linked promotion of amyloid β and *tau* protein aggregates formulation in Alzheimer's disease (AD) [1], have a chance to be tested in such a model.

AD is a complex irreversible neurodegenerative disease triggered by several factors, such as, amyloidal plaques, cholinesterases abnormal activity and oxidative stress. Cholinesterases degrade the crucial cognitive functions neurotransmitter, acetylcholine, the amount of which is reduced by the progressively decreasing number of cholinergic neurons. Currently, only four drugs that are the acetylcholinesterase (AChE) inhibitors, donepezil, galantamine, and rivastigmine, and the glutamate NMDA receptor antagonist, memantine, are used as a standard of care for AD treatment. However, new therapeutic strategies are being developed to reach other causes of AD and make therapy more successful [2].

Amyloid beta (Aβ), with 40 and 42 amino acids in the chain, and *tau* protein aggregates are the leading cause of developing neurodegenerative diseases. Research indicates that the amyloid consisting of 42 amino acids (Aβ42) has the highest aggregation propensity and easily forms oligomers and fibrils [2]. The shorter protein consisting of 40 amino acids (Aβ40) was revealed to form predominantly monomeric structures [3]. Both the Aβ42 and Aβ40 are a source of inflammatory factors and reactive oxygen species [4]. Moreover, they cause an increase in acetylcholinesterase (AChE) and butyrylcholinesterase (BuChE) levels [5], as well as γ-aminobutyric acid (GABA)-ergic [6], dopaminergic and glutamatergic [7] neurotransmission inhibition. *Tau* protein, the major microtubule-stabilizing protein of a mature neuron, when hyperphosphorylated, decreases its solubility, hence promoting the formation of insoluble paired helical filaments (PHF) and tangles [8].

Medical practice shows that it is challenging to achieve satisfying AD therapy results with single-target drugs, thus

* **Corresponding author**
e-mail: kskalicka@pharmacognosy.org

© 2022 Author(s). This is an open access article distributed under the Creative Commons Attribution-NonComercial-No Derivs licence (http://creativecommons.org/licenses/by-nc-nd/3.0/)

multitarget remedies are considered to be a better treatment option [9]. Coumarins may be considered as multitargeted agents in the sense of AD therapy as they are reported to act as antioxidants and cholinesterase inhibitors with a high possibility to inhibit Aβ40/42/*tau* protein aggregation [1].

The activity of coumarins vary depending on the structure. Substitution of the simple coumarin in the C-7, C-4 and C-2 positions by hydroxyl (–OH) group gives high antioxidative properties. The C-7 position was found to be crucial for high-intensity antioxidative activity, while the C-4 position is known to be essential for initiating antioxidative reactions [10]. In contrast, replacing the –OH group with the -CH3 group in the C-4 position diminishes these properties [11]. Coumarins possessing -OH groups react with free radicals and inhibit chain reactions. They are also considered to be potent metal chelators and, therefore, would be benefitial in AD treatment, where a high concentration of free radicals and copper ions accumulation are reported [12] (Fig. 1, Fig. 2).

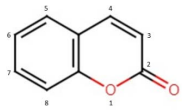


Figure 1. A simple coumarin, 1, 2-benzopyrones, with numbered carbons in the structure

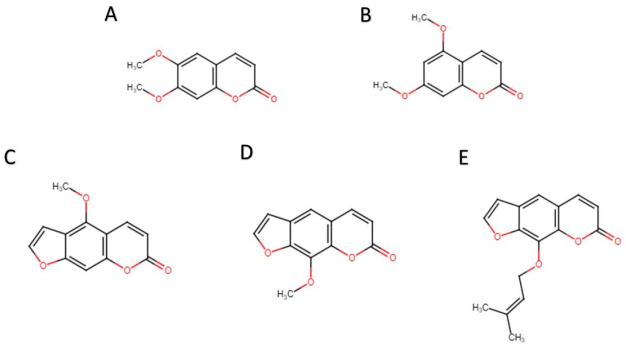


Figure 2. Comparison of the structure of selected coumarins A. Simple coumarin; scoparone (6,7-Dimethoxycoumarin), B. Simple coumarin; Limettin (5,7-dimethoxycoumarin), C. Linear furanocoumarin; Bergapten (5-methoxypsoralen), D. Linear furanocoumarin; Xanthotoxin (8-methoxypsoralen), E. Linear furanocoumarin; Imperatorin (8-isoamylenoxypsoralen)

For the current study, two simple coumarins (scoparone, limettin) and two furanocoumarin analogs (bergapten, xanthotoxin) were selected in order to to compare the influence of the substituted groups on anti-AD activity. Additionally, another furanocoumarin, imperatorin, with an isoamylenoxy group, was included, as such a long aliphatic chain may dramatically change the pharmacological functions, as proved in our previous studies [13]. The present project aimed to investigate Aβ40/42 and *tau* structure-dependent inhibiting properties of selected coumarin analogs and demonstrate the multitargeted character of these drugs in AD by way of the rapid screening method via the bacteria cell model of AD [14]. The above-mentioned screening method was used for the first time in this study to evaluate the coumarins' neuroprotective activities.

MATERIALS AND METHODS

Compounds

Limettin, bergapten, and xanthotoxin were purchased from Sigma Aldrich. As described previously, scoparone was isolated from *Artemisia umbelliformis* Lam. (*Asteraceae*) [15]. Imperatorin was isolated as described previously [16].

Coumarin influence upon the Aβ42 peptide and on *tau* protein aggregation *in cellulo*

Bacterial model of AD

Scoparone, limettin, bergapten, xanthotoxin and imperatorin stock solutions were prepared by dissolving in dimethyl sulfoxide (DMSO) and sonicated. The stock solution (200 mM) was then dissolved in MiliQ water (Merck-Millipore, USA) and sequential dilutions were performed (2, 4, 10, 20, 50, 100, 200, 250, 500, 750, 1000, 2500 µM). The concentrations were chosen experimentally.

Cloning and over-expression of Aβ42 peptide

Escherichia coli (*E. coli*) competent cells – strain BL21 (DE3), were transformed with the pET28a vector (Novagen, Inc., Madison, WI, USA) carrying the DNA sequence of Aβ42, as described previously [14].

As a negative control (maximal amyloid presence), the same amount of DMSO without drug was added to the sample. In parallel, non-induced samples (in the absence of isopropyl ß-D-1-thiogalactopyranoside (IPTG)) were also prepared and used as positive controls (non-amyloid presence). In addition, these samples were used to assess the compounds' potential intrinsic toxicity and confirm the correct bacterial growth.

Cloning and overexpression of tau protein

E. coli BL21 (DE3) competent cells were transformed with pTARA containing the RNA-polymerase gene of T7 phage (T7RP) under the control of the promoter PBAD. In addition, *E. coli* BL21 (DE3) with pTARA competent cells were transformed via the pRKT42 vector so as to encode four repeats of *tau* protein in two inserts. The following steps were conducted as described above. Minimal medium (M9) contained 50 $\mu g \cdot mL^{-1}$ of ampicillin and 12.5 $\mu g \cdot mL^{-1}$ of chloramphenicol. When the cell density reached OD_{600} = 0.6, an amount of 980 µL of culture was transferred into Eppendorf tubes of 1.5 mL, with 10 µL of each compound to be tested in DMSO and 10 µL of arabinose at 25%. For IC_{50}, the same protocol is followed, only modifying the initial concentration of each compound.

As a negative control (maximal presence of *tau*), the same amount of DMSO without drug was added to the sample. In parallel, non-induced samples (in the absence of arabinose) were also prepared and used as positive controls (absence of *tau*). The cell viability was checked as described above.

Thioflavin S fluorescence determination

Thioflavin S, a fluorescent compound, emits fluorescence with an excitation peak at 391 nm and an emission peak at 428 nm. Thioflavin S (Th-S) fluorescence and absorbance were tracked using a DTX 800 plate reader Multimode

Detector equipped with Multimode Analysis Software (Beckman-Coulter, USA) with filters of 430/35 and 485/20 nm for the excitation and emission wavelengths, respectively. The detection was done as described previously [14].

In vitro Aβ42 aggregation assay

Aβ42 was provided from Bachem (Switzerland) and *in vitro* analysis was performed as described previously [14]. For aggregate-free preparation, Aβ42 (5 mg) was solubilized in 1,1,1,3,3,3-hexafluoro-2-propanol (HFIP; 2 mL) under vigorous stirring, sonication aliquoting and HFIP evaporation, and stored at -33ºC. Next, the dry fraction was dissolved in 50 µl of DMSO, sonicated and 850 µL of native buffer (50 mM Tris, 150 mM NaCl, pH 7.4) was added. Subsequently, 3 µl of stock solution of scoparone was added to obtain a final concentration of 300 µM (IC_{50} indicated in the first stage of the project). The same volume of DMSO was added to the sample for the control samples. Samples were kept 48 hours in the Thermomixer at 3°C and 1400 rpm.

The negative control was kept in a refrigerator (2-8°C) overnight to stop aggregation. Right before the detection, 20 µL of thioflavin T (Th-T) at 250 µM was added to each sample.

Thioflavin T fluorescence determination

Thioflavin T is a dye that shows enhanced fluorescence on binding to amyloid formations *in vitro*. An Aminco Bowman Series 2 luminescence spectrophotometer, using an excitation wavelength of 445 nm and emission range from 460 nm to 600 nm was employed in this work. The amyloid peak, at 485 nm, was used to evaluate and quantify the amyloid concentration. The applied parameters and procedures were described previously by Espargaró *et al*. [14].

Aβ aggregation kinetic assays

For *in vitro* assays, Aβ aliquots were re-suspended in 50 µL of DMSO, and the monomers were solubilized using sonication for 10 min. The volume was completed to 1000 µL with Tris buffer (50 mM Tris, 150 mM NaCl, pH 7.4) containing 25 mM ThT and 10 µM of the drug. 200 µL of the samples were placed in a 96-well plate at 37°C and stirred at 700 rpm with double orbital mode. The course of the aggregation was followed by ThT fluorescence using a FLUOstar OMEGA plate reader (BMG Labtech GmbH), equipped with excitation and emission filters (λ_{exc} 440 nm; λ_{em} 490 nm). The amyloid aggregation was considered an autocatalytic reaction characterized by nucleation (k_n) and elongation (k_e) constants.

Extrapolation of the linear portion of the sigmoid curve to the abscissa and to the highest ordinate of the fitted plot gives two values, i.e., t_0 and t_1, corresponding to the lag time and end-of-reaction time, respectively. The time of half-aggregation was defined as $t_{1/2}$ [14].

For *in cellulo* assays, the samples were prepared following the same protocol described above, and after following the same protocol described here for *in vitro* kinetic assays [17].

Statistical analysis

Statistical analysis was performed using GraphPad Prism 8.3.0 for OS X. One-way ANOVA analysis with the post hoc Tukey's test ($p < 0.05$) was used to evaluate statistical significance. To determine the IC_{50} values of the tested coumarins, a sigmoidal dose-response (variable slope) equation in GraphPad Prism 8.3.0 for OS X was used. The graphs show the results as mean ± SEM indicated from the average of 10-5 individual assays.

The results from the use of the Aminco Bowman Series 2 luminescence spectrophotometer were pictured in graphs as a correlation of aggregation inhibition to log[compound].

RESULTS

Inhibitory effect of tested coumarins on Aβ42 peptide and *tau* aggregation

In cellulo assays at a fixed concentration

As shown in Table 1, the inhibitory activity of compounds tested at 100 µM ranges from 17.1 to 34.0 %, the potency of which decreases in the manner: bergapten > scoparone > limettin > imperatorin > xanthotoxin. The most potent, the weakest inhibitors of Aβ42 and a structural derivative with the longest aliphatic chain, bergapten, xanthotoxin and imperatorin respectively, were chosen to evaluate inhibiting potency towards *tau* protein. The *tau* aggregation inhibition analysis aligns with the results obtained for Aβ42. However, the *tau* protein inhibiting activity was noticeably weaker than that for Aβ42, albeit with the same decreasing manner of inhibiting potency: bergapten > imperatorin > xanthotoxin (Tab. 1).

Table 1. Effect of anti-aggregating compounds (100 µM) monitored by Th-S staining of bacterial cells overexpressing Aβ42 peptide and *tau* protein

Compound	Aβ42 Inhibition (%)	SEM	*tau* inhibition (%)	SEM
Control	0.0	2.1	0.0	1.9
Scoparone	29.8	5.2	-	-
Limettin	23.8	2.3	-	-
Bergapten	34.0	2.9	16.3	2.2
Xanthotoxin	17.1	1.7	8.4	1.5
Imperatorin	21.9	2.6	14.4	3.1

Half-maximal inhibitory concentration (IC_{50}) determination *in cellulo* assays

Since at 100 µM selected coumarins display discrete effectivity, we determined the IC_{50} for Aβ42 aggregation for scoparone, limettin and imperatorin – compounds that showed similar inhibition potency.

As shown in Figure 3, the inhibition of Aβ42 increased with the higher doses. Figure 3A reveals the tendency of changes in Aβ42 aggregation inhibition (%) *vs*. scoparone concentration (log[scoparone]) in concentrations that ranged from 0 to 2500 µM in a sigmoidal dose-response (variable slope). Herein: IC_{50} = 319.8 µM; $LogIC_{50}$ = 2.505; (number of points: X values = 32; Y values analysed = 16; 95% CI (asymptotic): $LogIC_{50}$ = 2.449 to 2.561; HillSlope

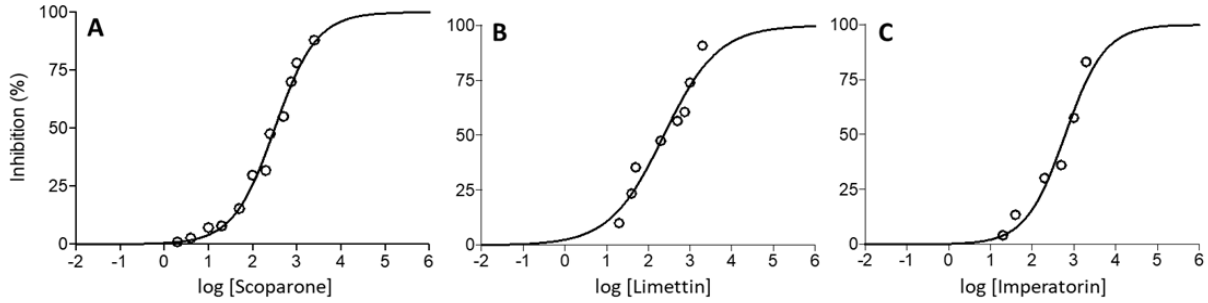


Figure 3. Anti-aggregating effect of coumarins monitored by Th-S staining of bacterial cells overexpressing Aβ42 peptide inhibition (%) *vs*. log[drug]. In A) Scoparone, B) Limettin, and C) Imperatorin

= 0.7996 to 1.038; IC_{50} = 280.9 μM to 364.1 μM. Figure 3B illustrates the tendency of changes in Aβ42 aggregation inhibition (%) *vs*. limettin concentration (log[limettin]) in a concentration range from 0 to 2000 μM in sigmoidal dose-response (variable slope), wherein: IC_{50} = 236.2 μM; LogIC50 = 0.06561; (number of points: X values = 28; Y values analysed = 12; 95% CI (asymptotic): 2.227 to 2.519; HillSlope = 0.5044 to 0.8336; IC_{50} = 168.7 μM to 330.7 μM. Finally, Figure 3C displays the tendency of changes in Aβ42 aggregation inhibition (%) vs. imperatorin concentration (log[imperatorin]) in a concentration range from 0-2000 μM in sigmoidal dose-response (variable slope) that indicated: IC_{50} = 623.9 μM; $LogIC_{50}$ = 2.795; (number of points: X values = 26; Y values analysed = 10; 95% CI (asymptotic): 2.667 to 2.923; HillSlope = 0.6225 to 1.209; IC_{50} = 464.7 μM to 837.7 μM. Accordingly, scoparone and limettin showed almost twice lower IC_{50} value compared to imperatorin. It could hence be concluded that simple coumarins are stronger inhi-bitors of Aβ42 aggregation than furanocoumarins (Fig. 3).

As previously published, the fibrils aggregation inhibition capacity of anti-amyloid compounds is usually similar for both Aβ42 and *tau* [18]. Since scoparone, limettin and imperatorin displayed IC_{50} of 319.8, 236.2, and 623.9 μM in the Aβ42 assays, the concentrations of 300, 250 and 600 μM (respectively), were considered as potentially effective in the *tau* assays. As shown in Table 2, the inhibition activity of the tested coumarins against *tau* is 50% higher than expected. In summary, the selected compounds possess much stronger *tau* than Aβ42 inhibition properties, wherein furanocoumarin and imperatorin, the weakest Aβ42 inhibitors, become the most effective coumarin in this assay (87%) (Tab. 2).

Table 2. Anti-aggregating effect of scoparone (300 μM), limettin (250 μM), and imperatorin (600 μM) monitored by Th-S staining of bacterial cells overexpressing full-length *tau* protein

DRUG [mM]	*In-cellulo* Inhibition (%)	SEM
Control	0.0	3.8
Scoparone [300 μM]	80.0	3.7
Limettin [250 μM]	67.4	6.5
Imperatorin [600 μM]	87.0	1.9

Effect of coumarins *in cellulo Aβ42 aggregation kinetics*

Since the previous assays with higher doses show unexpected inhibition results, further *in cellulo* kinetic analysis with Aβ42 was performed to investigate the manner of changes in time that occurred when using the lower dose of 10 μM. As shown in Figure 4 and Table 3, the lag time (t_0) for scoparone and limettin was increased by 47 and 36.5 minutes, respectively, compared to the control group. This outcome may suggest the occurrence of an interaction between Aβ42 soluble species, *viz*. monomer, nucleus or oligomers, the outcome of which results in a delay in the nuclei formation.

Table 3. Kinetic parameters of Aβ42 amyloid aggregation in the absence and presence of scoparone and limettin

Inhibitor	Control	Scoparone	Limettin
k_n (min^{-1})	7.76E^{-05}	7.91E^{-05}	1.42E^{-05}
k_e^{app} ($M^{-1}\cdot min^{-1}$)[a, b]	1459.2	1437.0	2336.7
t_0 (min)	303.6	340.1	350.6
$t_{1/2}$ (min)	530.9	506.8	489.5
t_1 (min)	758.1	673.4	628.4
Inhibition (%)	0.0	6.1	14.6

Table 3 shows inhibition specification at 10 μM of inhibitor. [a] Since Aβ42 concentration is not constant along the aggregation process, the k_e is apparent. [b] In order to calculate the k_e^{app}, as previously published [20], a final Aβ42 concentration has been considered. k_n (min^{-1}) describes nucleation constant; k_e ($M^{-1}\cdot min^{-1}$) describes elongation constant; t_0 (min) describes the start point of aggregation and the lag time; $t_{1/2}$ (min) describes half time; t_1 (min) describes the end time; inhibition (%) describes the maximum of aggregation inhibition

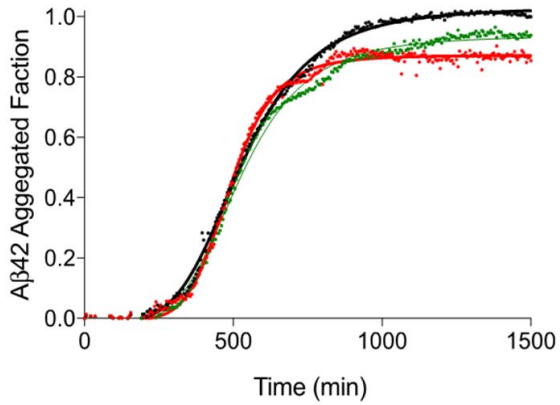


Figure 4. *In cellulo* Aβ42 aggregation kinetic in the absence (in black) and presence of scoparone (in green) and limettin (in red) (10 μM)

In contrast, reductions in half time ($t_{1/2}$) by 41.4 minutes, as well as in end time (t_1) by 129.7 for limettin could envisage the acceleration of the fibril elongation. The nucleation constant (k_n) shows a reduction caused by limettin, suggesting a delay in the initiation of the nucleation process and significant interactions between soluble Aβ42 species. In contrast, scoparone's nucleation constant (k_n) is practically unaltered, suggesting negligible interaction with soluble Aβ42 species. The elongation constants (k_e) present the acceleration of Aβ42 fibrils elongation by limettin by 0.62-fold and an almost lack of scoparone effect (1.01-fold) on the Aβ42 fibril formation processes. Even though limettin accelerates the fibril elongation, no effect is observed in the presence of scoparone. Thus, kinetic data confirms different inhibition mechanisms for the tested simple coumarins (Fig. 4, Tab. 3).

As shown in Figure 5 and Table 4, bergapten revealed 2.6 times and 3.8 times a more substantial effect on Aβ42 than xanthotoxin (8.1%) and imperatorin (5.6%), respectively. Interestingly, bergapten presented a more advantageous kinetic profile than xanthotoxin and imperatorin, wherein the lag time was prolonged by 53.6 minutes, suggesting a significant delay in the initiation of nucleation processes. Moreover, the nucleation constant (k_n) was reduced, indicating that it holds the most potent capacity of interacting with the soluble Aβ42 species by delaying the first nucleation events. In contrast, the lag time for xanthotoxin was reduced by 29.2 minutes compared to the control group, envisaging a premature initiation of nucleation processes (Fig. 5, Tab. 4).

Table 4. Kinetic and kinetic parameters of Aβ42 amyloid aggregation affected by bergapten, xanthotoxin, and imperatorin

Inhibitor	Control	Bergaptena	Xanthotoxina	Imperatorin
k_n (min^{-1})	7.76E^{-05}	2.84E^{-05}	8.50E^{-05}	5.41E^{-05}
k_e^{app} ($M^{-1}\cdot min^{-1}$)^{a,b}	1459.2	1901.7	1603.3	1790.0
t_0 (min)	303.6	356.8	274.4	303.8
$t_{1/2}$ (min)	530.9	513.1	491.8	476.2
t_1 (min)	758.1	669.3	709.2	648.6
Inhibition (%)	0.0	21.4	8.1	5.6

Table 4 shows inhibition specification at 10 μM of inhibitor. [a] Since Aβ42 concentration is not constant along the aggregation process, the k_e is apparent. [b] In order to calculate the k_e^{app}, as previously published [20], a final Aβ42 concentration of Aβ42 has been considered. k_n (min^{-1}) describes nucleation constant; k_e ($M^{-1}\cdot min^{-1}$) describes elongation constant; t_0 (min) describes the start point of aggregation and the lag time; $t_{1/2}$ (min) describes half time; t_1 (min) describes the end time; inhibition (%) describes the maximum of aggregation inhibition

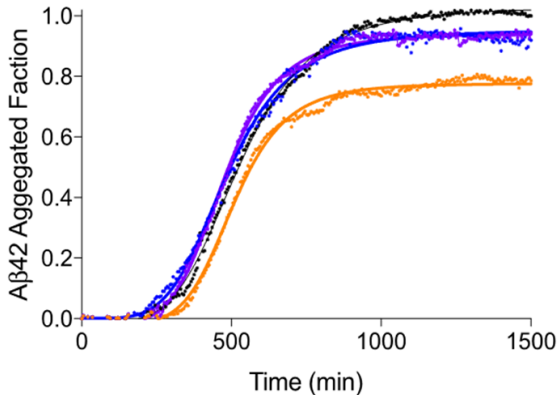


Figure 5. *In cellulo* Aβ42 aggregation kinetics in the absence (in black) and presence of 10 μM of bergapten (in orange), xanthotoxin (in blue), and imperatorin (in purple)

Effect of coumarins *in vitro* Aβ40 aggregation kinetics

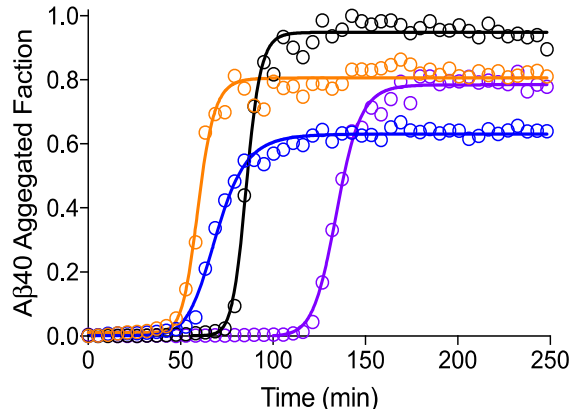
Since the Aβ40 peptide displays more reproducible aggregation kinetics *in vitro* than Aβ42, the *in vitro* kinetic assay was performed using the Aβ40 peptide.

Figure 6 and Table 5 show a lag time reduction by 27.1 and 24.8 minutes by bergapten and xanthotoxin, respectively. This suggests premature initiation of interactions between Aβ40 soluble species, *viz*. monomer, nucleus or oligomers, that involves the formation of hetero-nuclei and a triggering of the protein aggregation, but not necessary in amyloid conformation [14,17]. In contrast, an increase in the lag time by 43.6 minutes caused by imperatorin suggests delated aggregation initiation [14]. Declines in aggregation half time ($t_{1/2}$) are 26.2 and 16.7 minutes, and that in the end time (t_1) are 25.4 and 8.7 minutes for bergapten and xanthotoxin, respectively, indicate the acceleration of the fibril elongation. In contrast, imperatorin induced increments in aggregation half time ($t_{1/2}$) by 49.1 minutes and in end time by 62.9 minutes (t_1), demonstrate a delay in the fibril formation and elongation processes [14,17]. This outcome suggests that Aβ40 soluble monomers in the presence of imperatorin show less affinity to bind to nuclei.

Table 5. Kinetic parameters of Aβ40 amyloid aggregation in the absence and presence of bergapten, xanthotoxin, and imperatorin

Inhibitor	Control	Bergapten	Xanthotoxin	Imperatorin
k_n (min^{-1})	2.42E^{-09}	6.50E^{-06}	7.54E^{-05}	2.09E^{-09}
k_e ($M^{-1}\cdot min^{-1}$)	14066.7	11126.7	6680.0	8800.0
t_0 (min)	77.5	50.4	52.7	121.1
$t_{1/2}$ (min)	85.9	59.7	69.2	135.0
t_1 (min)	94.4	69.0	85.7	148.8
Inhibition (%)	0.0	13.7	33.3	17.5

[Drugs] = 10 μM; [Aβ40] = 15 μM



[Aβ40] = 15 μM

Figure 6. *In vitro* Aβ40 aggregation kinetics in the absence (in black) and presence of 10 μM of bergapten (in orange), xanthotoxin (in blue), and imperatorin (in purple)

Our work demonstated that xanthotoxin inhibited Aβ40 aggregation almost 2.4 and 1.9 times stronger than its structural analogs, bergapten and imperatorin, respectively. Furthermore, both bergapten and xanthotoxin caused an indicative increase in the nucleation constant (k_n), suggesting significant drug-soluble species interactions entailing the acceleration of Aβ40 aggregation toward non-amyloid

pathways. In addition, reductions of elongation constant (k_e) by 1.3-fold, 2.1-fold, and 1.6-fold were demonstrated by the application of bergapten, xanthotoxin, and imperatorin, respectively, indicate drug-Aβ40 fibrils formation interactions that entail reduction of the fibril elongation (Fig. 6, Tab. 5).

As shown in Figure 7 and Table 6, limettin and scoparone, although simple coumarins, act as the most potent Aβ40 aggregation inhibitors (61.9% and 41.3%, respectively), whereas the furanocoumarins – bergapten, xanthotoxin and imperatorin – were much weaker (13.7%, 33.3%, and 17.5%, respectively). However, different inhibitory mechanisms can be envisaged from the kinetic data. Whereas scoparone displays a slight reduction in lag time with a threefold reduction in the fibril elongation, limettin displays a slight increment in the nucleation constant with also a significant reduction in the elongation constant (Fig. 7, Tab. 6).

Table 6. Kinetic parameters of Aβ40 amyloid aggregation in the absence and presence of scoparone and limettin

Inhibitor	Control	Scoparone	Limettin
k_n (min^{-1})	2.42E^{-09}	6.05E^{-05}	1.48E^{-08}
k_e ($M^{-1}\cdot min^{-1}$)	14066.7	5480.7	6336.0
t_0 (min)	77.5	68.0	147.5
$t_{1/2}$ (min)	85.9	85.4	162.4
t_1 (min)	94.4	102.8	177.3
Inhibition (%)	0.0	41.3	61.9

[Drugs] = 10 μM; [Aβ40] = 15 μM

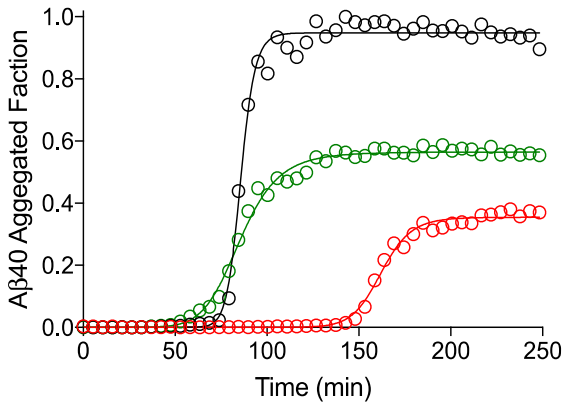


Figure 7. *In vitro* Aβ40 aggregation kinetics in the absence (in black) and presence of 10 μM of scoparone (in green) and limettin (in red). [Aβ40] = 15 μM

DISCUSSION

Since scoparone, limettin, bergapten, xanthotoxin and imperatorin exert different procognitive mechanisms, as revealed in the previous studies [13,15], they were selected for the fast screening of inhibitory activity towards Aβ40/42 (*in vitro/in cellulo*) and *tau* protein aggregation so as to compare Aβ40/42 inhibiting potential with their structural variations.

In the preliminary study, limettin (IC_{50} = 250 μM), scoparone (IC_{50} = 319.8 μM) and bergapten (at the dose of 100 μM (Tab. 1) showed themselves to be promising Aβ42 aggregation inhibitors. Kinetic analysis suggests that bergapten, imperatorin and limettin interacted with soluble Aβ42 species *in cellulo*, delaying the nucleation events (k_n) but accelerating the fibril elongation (k_e). The whole process ended prematurely (t_0) for furanocoumarin, bergapten and the simple coumarin, limettin. Based on *k*n and *k*e constants, we may suggest that coumarins tend to interact with soluble Aβ42 species *in cellulo* forming complexes with higher affinity for soluble Aβ monomers than Aβ-nuclei and fibrils. Of note: some studies have claimed that the soluble oligomeric intermediates are a primary cause of the toxicity of Aβ rather than the accumulation of insoluble fibrils [18,]. Indeed, soluble oligomeric intermediates may disrupt neuronal depolarization and repolarization abilities [19], long-term potentiation capacity [19], neuronal microRNA expression [20], and thus memory formation possibilities [19]. Oligomers vary in size and shape and are difficult to characterize, given their transient nature [18]. However, further studies are required to confirm the exact mechanism of coumarin action on soluble oligomers species.

The derived limettin kinetic constants (k_n) reveal the nucleation inhibition of both Aβ40 (*in vitro*) and Aβ42 (*in cellulo*). Moreover, limettin *in vitro* was found to have inhibited the intensity of Aβ40 fibril elongation (k_e) when compared to the control group (t_1). This action, therefore, might be crucial in countering the early stage of Aβ aggregates formation. We also observed that limettin, similar to the other tested coumarins (with exception of bergapten), exerted stronger Aβ40 (*in vitro*) than Aβ42 aggregation (*in cellulo*). Previous work has demonstrated that amyloidal plaques mainly consist of Aβ40 than Aβ42 type of amyloidal proteins [21]. Moreover, the concentration of Aβ40 in the cerebral spinal fluid has been found to be several-fold more abundant than that of Aβ42 [22]. The study by Lei Gu and Zhefeng Guo suggests that Aβ42 and Aβ40 monomers interact with each other in the process of aggregation, and thus a coexistence of Aβ42 and Aβ40 in the extracellular space may generate aggregates containing three populations: Aβ42 alone, Aβ40 alone, and Aβ42/Aβ40 mix [23]. Although it is clear that Aβ40 plays a role in the process of fibril formation, further studies are required to investigate the exact mechanism of its action in AD pathogenesis.

Contrary to limettin, its analog, scoparone, exerted a weaker effect on both proteins. In addition, Aβ40/42 (*in vitro/in cellulo*) protein soluble species-scoparone interactions were weak and we may claim that there was no inhibition of oligomers formation. This outcome shows that the substitution of the C-6 position changes the mechanism of action of simple coumarins.

A furanocoumarin, bergapten, exerted the most potent Aβ42 inhibition *in cellulo*, which was 1.56-times stronger than the inhibition of the Aβ40 aggregation *in vitro*. In contrast to bergapten, its analog, xanthotoxin, showed Aβ42 (*in cellulo*) and Aβ40 (*in vitro*) nucleation events intensification and premature initiation of aggregation, elongation and fibril formation events. We conclude that the -OCH3 group in the C-8 position deteriorates the inhibitory effect on Aβ40/42 soluble species interactions and fibril formation processes.

We found that changing the -OCH3 in the C-8 position in furanocoumarins on the isoamylenoxy group slowed down Aβ40 nucleation events *in vitro* and delayed the initiation

of aggregation. This result shows that a longer aliphatic chain in the C-8 position interrupts soluble species interaction. However, further studies are required to explain the imperatorin mechanism of action.

Coumarin structure-activity relationship analysis revealed that the C-6 and C-8 substitution influenced anti-AChE function and anti-Aβ aggregation [23]. Artanin and limettin are structurally alike with the difference being in the isoamylenoxy chain in the C-8 position in the artanin structure. Artanin (IC_{50} = 124 μM) seems to be a more potent Aβ42 aggregation inhibitor than limettin (IC_{50} = 236.2 μM), which suggests that a long aliphatic chain increases the inhibiting potency of simple coumarins [23].

The weaker inhibitory activity of tested coumarins towards Aβ42 (*in cellulo*) than Aβ40 (*in vitro*) aggregation was not fully explained in our work. This can be considered as a limitation of the study. The substituted groups may possibly modify the activity of the specific coumarin derivative and the transferability through the bacterial cell membrane might have limited the effectivity of tested coumarins *in cellulo* assays of Aβ42 aggregation.

CONCLUSIONS

As revealed in the present project, limettin and imperatorin may effectively delay the nucleation process, which is the first step of amyloidal aggregation, and delay fibril formation/elongation processes. Thus, limettin and imperatorin might be potent Aβ40 inhibitors. Importantly, most of the tested coumarins showed more potent inhibitory activity towards Aβ40 – which might be a significant feature in further studies. Also, our findings suggest that coumarin derivatives could be modified to intensify their antiamyloidal properties, as our work has demonstrated the influence of the length of the aliphatic chain and the place of substitution. All in all, the present study indicates that natural compounds are a good basis for designing new multitarget drugs that could be used in either the prevention or treatment of AD.

LIST OF ABBREVIATIONS

Aβ – Amyloid-beta
Aβ42 – amyloid consisting of 42 amino acids
Aβ40 – amyloid consisting of 40 amino acids
AChE – acetylcholinesterase
AD – Alzheimer's disease
L21 DE3 – strain of Escherichia coli competent cells
BuChE – butyrylcholinesterase
DMSO – dimethyl sulfoxide
E. coli – *Escherichia coli*
GABA – γ-aminobutyric acid
IC_{50} – half-maximal inhibitory concentration
IPTG – isopropyl ß-D-1-thiogalactopyranoside
k_e – elongation constants
k_n – nucleation constant
M9 – Minimal medium
PHF – insoluble paired helical filaments
Thioflavin S fluorescence – fluorescence that is emitted by Thioflavin S
Thioflavin T fluorescence – fluorescence that is emitted by Thioflavin T
T7RP – RNA-polymerase gen of T7 phage
Th-S – Thioflavin S
Th-T – Thioflavin T
t_0 – lag time
$t_{1/2}$ – half time
t_1 – end tim

FUNDING

This study was supported by grant no. 2017/27/B/NZ4/00917 from National Science Center, Poland

ORCID iDs

Joanna Kowalczyk https://orcid.org/0000-0002-4872-250X
Krystyna Skalicka-Woźniak https://orcid.org/0000-0002-9313-5929
Barbara Budzynska https://orcid.org/0000-0001-5917-9285
Nesrine El Sayed https://orcid.org/0000-0002-7912-3913
Alba Espargaró https://orcid.org/0000-0001-6739-767X
Raimon Sabaté https://orcid.org/0000-0003-3894-2362

REFERNCES

1. Serrano-Pozo A, Das S, Hyman BT. APOE and Alzheimer's disease: Advances in genetics, pathophysiology, and therapeutic approaches. *Lancet Nerol*. 2021;20(1):68-80.
2. Hardy J, Selkoe DJ. The amyloid hypothesis of Alzheimer's disease: progress and problems on the road to therapeutics. *Science*. 2002; 297:353-6.
3. Dasari M, Espargaro A, Sabate R, Lopez Del Amo JM, Fink U, Grelle G, et al. Bacterial inclusion bodies of Alzheimer's disease β-amyloid peptides can be employed to study native-like aggregation intermediate states. *Chembiochem*. 2011;12:407-23.
4. Mao P, Reddy PH. Aging and amyloid beta-induced oxidative DNA damage and mitochondrial dysfunction in Alzheimer's disease: implications for early intervention and therapeutics. *Biochim Biophys Acta*. 2011;1812:1359-70.
5. Govoni S, Mura E, Preda S, Racchi M, Lanni C, Grilli M, et al. Dangerous liaisons between beta-amyloid and cholinergic neurotransmission. *Curr Pharm Des*. 2014;20:2525-38.
6. Tang BL. Amyloid Precursor Protein (APP) and GABAergic neurotransmission. *Cells*. 2019;8:550.
7. Girek M, Szymański P. Tacrine hybrids as multi-target-directed ligands in Alzheimer's disease: influence of chemical structures on biological activities. *Chem Papers*. 2018;73:269-89.
8. Morphy R, Rankovic Z. Designed multiple ligands. An emerging drug discovery paradigm. *J Med Chem*. 2005;48:6523-43.
9. Skalicka-Woźniak K, Orhan IE, Cordell GA, Nabavi SM, Budzyńska B. Implication of coumarins towards central nervous system disorders. *Pharmacol Res*. 2016;103:188-203.
10. Rao VR. *Antioxidant Agents. Advances in structure and activity relationship of coumarin derivatives*. London; 2016:137-50.
11. Wang L, Yin YL, Liu XZ, Shen P, Zheng YG, Lan XR, et al. Current understanding of metal ions in the pathogenesis of Alzheimer's disease. *Transl Neurodegener*. 2020;9 :10.
12. Budzynska B, Boguszewska-Czubara A, Kruk-Slomka M, Skalicka-Wozniak K, Michalak A, Musik I, et al. Effects of imperatorin on scopolamine-induced cognitive impairment and oxidative stress in mice. *Psychopharmacology* (*Berl*). 2015;232:931-42.
13. Espargaró A, Medina A, di Pietro O, Muñoz-Torrero D, Sabate R. Ultra rapid in vivo screening for anti-Alzheimer anti-amyloid drugs. *Scientific Reports*. 2016;6:1-8.
14. Kowalczyk J, Budzyńska B, Kurach Ł, Pellegata D, Sayed NS, Gertsch J, et al. Neuropsychopharmacological profiling of scoparone in mice. *Sci Rep*. 2022;12:822.
15. Kozioł E, Skalicka-Woźniak K. Imperatorin–pharmacological meaning and analytical clues: profound investigation. *Phytochem Rev*. 2016;15:627-49.
16. Espargaró A, Sabaté R, Ventura S. Kinetic and thermodynamic stability of bacterial intracellular aggregates. *FEBS Letters*. 2008;582: 3669-73.

17. Espargaró A, Pont C, Gamez P, Muñoz-Torrero D, Sabate R. Amyloid pan-inhibitors: One family of compounds to cope with all conformational diseases. *ACS Chem Neurosci*. 2019;10:1311-7.
18. Lue LF, Kuo YM, Roher AE, Brachova L, Shen Y, Sue L, et al. Soluble amyloid β peptide concentration as a predictor of synaptic change in Alzheimer's disease. *Am J Pathol*. 1999;155:853-62.
19. Walsh DM, Klyubin I, Fadeeva JV, Cullen WK, Anwyl R, Wolfe MS, et al. Naturally secreted oligomers of amyloid beta protein potently inhibit hippocampal long-term potentiation *in vivo*. *Nature*. 2002;416:535-9.
20. Li JJ, Dolios G, Wang R, Liao FF. Soluble beta-amyloid peptides, but not insoluble fibrils, have specific effect on neuronal microRNA expression. *PLoS One*. 2014;9(3):e90770.
21. Yang J, Zhu B, Yin W, Han Z, Zheng C, Wang P, et al. Differentiating Aβ40 and Aβ42 in amyloid plaques with a small molecule fluorescence probe. *Chem Sci*. 2020;11:5238-45.
22. Gu L, Guo Z. Alzheimer's Aβ42 and Aβ40 peptides form interlaced amyloid fibrils. *J Neurochem*. 2013;126:305.
23. Takomthong P, Waiwut P, Yenjai C, Sripanidkulchai B, Reubroycharoen P, Lai R, et al. Structure-activity analysis and molecular docking studies of coumarins from Toddalia asiatica as multifunctional agents for Alzheimer's disease. *Biomedicines*. 2020;8(5):107.